

SUBSTITUTIONS IN THE DOMAIN III VOLTAGE SENSING MODULE ENHANCE THE SENSITIVITY OF AN INSECT SODIUM CHANNEL TO A SCORPION β -TOXIN

Weizhong Song¹, Yuzhe Du¹, Zhiqi Liu¹, Ningguang Luo¹, Michael Turkov²,
Dalia Gordon², Michael Gurevitz², Alan L. Goldin³, Ke Dong^{1†}

From the ¹Department of Entomology, Genetics Program and Neuroscience Program, Michigan State University, East Lansing, MI 48824; ²Department of Plant Molecular Biology and Ecology, George S. Wise Faculty of Life Sciences, Tel-Aviv University, Israel;

³Department of Microbiology and Molecular Genetics, University of California, Irvine, CA 92697

Address correspondence to:

†Ke Dong, Department of Entomology, Genetics Program and Neuroscience Program, Michigan State University, East Lansing, MI 48824. Tel: 517-432-2034; Fax: 517-353-4354; Email: dongk@msu.edu

Scorpion β -toxins bind to the extracellular regions of the voltage sensor module of domain II and to the pore module of domain III in voltage-gated sodium channels (Na_v channels), and enhance channel activation by trapping and stabilizing the voltage sensor of domain II in its activated state. We investigated the interaction of a highly potent insect selective scorpion depressant β -toxin, Lqh-dprIT₃, from *Leiurus quinquestriatus hebraeus*, with insect sodium channels (BgNa_v) from *Blattella germanica*. Like other scorpion β -toxins, Lqh-dprIT₃ shifts the voltage dependence of activation of BgNa_v channels expressed in *Xenopus* oocytes to more negative membrane potentials, but only after strong depolarizing prepulses. Notably, among 10 BgNa_v splice variants tested for their sensitivity to the toxin, only BgNa_v1-1 was hypersensitive due to an L1285P substitution in IIS1 resulting from a U-to-C RNA editing event. Furthermore, charge reversal of a negatively-charged residue (E1290K) at the extracellular end of IIS1, and the two innermost positively charged residues (R4E and R5E) in IIS4, also increased the channel sensitivity to Lqh-dprIT₃. Besides enhancement in toxin sensitivity, the R4E substitution caused an additional 20 mV negative shift in the voltage-dependence of activation of toxin-modified channels, inducing a unique toxin-modified state. Our findings provide the first direct evidence for the involvement of the domain III voltage sensing module in the action of

scorpion β -toxins. This hypersensitivity most likely reflects an increase in IIS4 trapping via allosteric mechanisms, suggesting the coupling between the voltage sensors in neighboring domains during channel activation.

Voltage-gated sodium channels (Na_v channels) are essential for the initiation and propagation of action potentials in most excitable cells. They consist of a large pore-forming α -subunit that is associated with a variable number of smaller subunits in different excitable tissues (1). The α -subunit comprises four repeat homologous domains (I-IV), each having six membrane spanning segments (S1-S6). The S1-S4 segments constitute the voltage sensing module. S4 in each domain contains four to seven positively charged residues and moves outward in response to membrane depolarization, which initiates the channel activation process (1). The S5 and S6 segments and their connecting P loops comprise the pore-forming module. Each reentrant P loop contains two short segments (SS1 and SS2) which span the membrane as hairpin and form the lining of the pore.

Mammals produce functionally and pharmacologically diverse Na_v α -subunits by selective expression of distinct sodium channel genes (at least nine in rat and human) in different tissues (2,3). In insects, such as *Drosophila melanogaster* and *Blattella germanica*, extensive

alternative splicing and RNA editing of a single gene generate a broad array of variants that are diverse in gating and pharmacological properties (4-6).

Due to their pivotal role in excitability, Na_v channels are targeted by a variety of toxins derived from plants and animals as part of their defense or preying strategies (1,7-10). Among venomous animals, scorpions produce a rich repertoire of 61-76 residue-long peptide toxins that modify sodium channel gating upon binding to distinct extracellular receptor sites in the α -subunit (7,8,11-13). The toxins that affect Na_v s are divided into α - and β -classes according to their mode of action and binding properties (14,15). α -toxins inhibit channel fast inactivation in a voltage-dependent manner upon binding at receptor site-3, assigned mainly to domains I and IV. β -toxins interact with receptor site-4, assigned to the voltage sensor module of domain II and the pore module of domain III, and shift the voltage-dependence of activation to more negative membrane potentials (11,16-19). The sensitivity of mammalian Na_v subtypes to scorpion β -toxins differs greatly. Rat brain ($\text{rNa}_v1.2$) and skeletal muscle ($\text{rNa}_v1.4$) channels are often more sensitive than the cardiac channel ($\text{rNa}_v1.5$) to β -toxins of South American scorpions such as *Css4* from *Centruroides suffusus suffusus*, and *Ts1* from *Tityus serulatus*, *TdVIII* from *T. discrepans* (16-20). Moreover, *Tz1* from *Tityus zulianus* is especially active at $\text{rNa}_v1.4$ compared to $\text{rNa}_v1.2$ and $\text{hNa}_v1.5$ (18).

The prominent activity of *Css4* on $\text{rNa}_v1.2$ and $\text{rNa}_v1.4$ compared to its very weak effect on $\text{rNa}_v1.5$ motivated Catterall and associates to analyze each of the 16 extracellular loops of $\text{rNa}_v1.5$ in the background of $\text{rNa}_v1.2$. Their analysis revealed that IS5-SS1, IIS1-S2, IIS3-S4 and IISS2-S6, particularly a G845N substitution in IIS3-S4, play a role in determining toxin preference, suggesting that scorpion β -toxins bind to the S3-S4 loop (16). In a similar fashion, differences in potency of the toxin *Tz1* on rat muscle, cardiac and neuronal Na_v s motivated swapping of $\text{rNa}_v1.2a$ sequences in the background of $\text{rNa}_v1.4$ by Heinemann and associates (18). This analysis revealed that three

amino acid residues in the C-terminal pore loop (SS2-S6) of domain III determine the *Tz1* preference for the skeletal muscle Na_v (18).

To account for enhanced sodium channel activation by *Css4*, a voltage-sensor trapping model was proposed in which the S4 voltage sensor of domain II (IIS4) is trapped and stabilized in its outward, activated position by the scorpion β -toxin (16,21). Neutralization or reversal of gating charges in the voltage-sensor of domain II enhances the action of scorpion β -toxins. According to the classical models of sodium channel gating, the voltage sensors of the sodium channel activate independently and at least three of them have to be in an activated position for the channel to open (22,23). In order for a scorpion β -toxin to shift the threshold of activation, more than one voltage-sensor could be affected by the toxins. Bezanilla and associates combined electrophysiological and spectroscopic measurements to determine the structural rearrangements induced by the scorpion β -toxin *Ts1* on the $\text{rNa}_v1.4$ channel (24). Consistent with studies using *Css4*, *Ts1* binding to the channel has been shown to be restricted to a single binding site in the voltage sensor of domain II where it traps IIS4 in the activated state. Interestingly, *Ts1* binding to S4 of domain II allosterically potentiates the activation of the other three voltage sensors at more hyperpolarized potentials. However, it is unknown how voltage-sensing modules in other domains contribute to the voltage sensor trapping by β -toxins.

In this study, we analyzed the sensitivity of 10 BgNa_v variants (25) to a potent insect-selective *Lqh-dprIT₃* depressant toxin (26). The discovery of one variant that is hypersensitive to *Lqh-dprIT₃* led to the identification of the critical effect of L1285 and E1290 in IIS1 on channel sensitivity to the toxin. We further show that substitutions of the two innermost positively-charged residues (R4E and R5E) in IIS4 also enhance the effect of *Lqh-dprIT₃*. These findings demonstrate that the voltage-sensing module of domain III is critical for the action of the scorpion β -toxin.

EXPERIMENTAL PROCEDURES

Toxin production and functional analysis. Of eight Lqh-dprIT₃ variants produced by the scorpion *Leiurus quinquestriatus hebraeus*, the highly potent variant-c, hereafter named Lqh-dprIT₃, was produced in recombinant form and analyzed as previously described (26).

Channel mutagenesis. Site-directed mutagenesis of BgNa_v1-1 and BgNa_v1-1a was performed via PCR using oligonucleotide primers and Pfu Turbo DNA polymerase (Stratagene, La Jolla, CA), and the modifications were verified by DNA sequencing.

Expression of BgNa_v channels in Xenopus oocytes. The procedures for oocyte preparation and cRNA injection are identical to those described previously (27). For robust expression of the BgNa_v channels, cRNA was coinjected into oocytes with *Drosophila melanogaster* tipE cRNA (1:1 ratio), which enhances channel expression (28,29).

Electrophysiological recording and analysis. The voltage-dependence of activation and inactivation was measured using the two-electrode voltage clamp technique. Methods for two-electrode recording and data analysis were similar to those described previously (30). Sodium currents were measured with a Warner OC725C oocyte clamp (Warner Instrument, Hamden, CT) and a Digidata 1322A interface (Axon Instruments Inc., Foster City, CA). Data were sampled at 50 kHz and filtered at 2 kHz. Leak currents were corrected by P/4 subtraction. pClamp 8.2 software (Axon Instruments Inc., CA) was used for data acquisition and analysis. The maximal peak sodium current was limited to <2.0 μA to achieve optimal voltage control.

The voltage dependence of sodium channel conductance (G) was calculated by measuring the peak current at test potentials ranging from -80 mV to +65 mV in 5 mV increments and divided by $(V - V_{\text{rev}})$, where V is the test potential and V_{rev} is the reversal potential for

sodium ions. Peak conductance values were normalized to the maximal peak conductance (G_{max}) and fit with a two-state Boltzmann equation of the form $G/G_{\text{max}} = [1 + \exp(V - V_{1/2})/k]^{-1}$, or with the sum of two such expressions, in which V is the potential of the voltage pulse, $V_{1/2}$ is the voltage for half maximal activation, and k is the slope factor.

The percentage of channel modification by Lqh-dprIT₃ was determined by the percentage of channels with the voltage-dependence of activation shifted to negative membrane potentials which was derived from double Boltzmann fits of the conductance-voltage relationships. Data were presented as mean ± S.D. Statistical significance was determined by one-way ANOVA ($p < 0.05$).

RESULTS

Effects of Lqh-dprIT₃ on sodium channel splice variant BgNa_v1-1. We first examined a well-characterized cockroach sodium channel BgNa_v1-1 (27) for the effect of Lqh-dprIT₃. Previous studies showed that for most of scorpion β-toxins, a strong depolarization prepulse is required for the toxins to induce a negative shift in the voltage-dependence of activation (11, 16-19). For example, a 1-ms depolarizing prepulse to 50 mV followed by a depolarizing test pulse to -65 mV activates Csx4-modified Na_v1.2 channels, but not unmodified channels (16). We initially used a similar protocol to examine the effect of Lqh-dprIT₃ on BgNav1-1 channels and found that a brief depolarizing pulse was not sufficient to detect Lqh-dprIT₃ action (data not shown). We then applied a 20-Hz train of 50 5-ms-depolarizing prepulses to 50 mV as the conditional pulses, followed by a 20-ms depolarizing test pulse between -80 mV and -65 mV from a holding potential of -120 mV. As expected, in the absence of the toxin, no sodium currents were detected under any of the test pulses (Fig. 1A). However, in the presence of 300 nM Lqh-dprIT₃, substantial sodium currents were detected at -75 mV to -65 mV (Fig. 1A), indicating Lqh-dprIT₃ modified the gating of BgNa_v1-1 channels.

The toxin effect was also evident in analyses of current-voltage relationship and conductance curves exhibiting a negative shift in the voltage dependence of channel activation after conditional prepulses in the presence of toxin (Fig. 1B, 1D). In addition, a significant increase in peak current was observed at 300 nM, but not at a lower concentration (100 nM) (Fig. 1B). Neither of these effects was observed without the prepulses (Fig. 1C). The voltage dependence of channel inactivation was not affected by the toxin (data not shown). At both 100 nM and 300 nM, the current-voltage and conductance-voltage relationships determined from Lqh-dprIT₃ effects were biphasic (Fig. 1D). Fitting of the conductance curves with the sum of two Boltzmann relationships revealed that the voltage dependence of activation of 40% (with 100 nM Lqh-dprIT₃) and 80% (with 300 nM Lqh-dprIT₃) of BgNa_v1-1 channels shifted 40 mV to a more hyperpolarizing membrane potential. The extent of the toxin-induced hyperpolarizing shift in activation was not concentration-dependent. Thus, like other scorpion β -toxins, Lqh-dprIT₃ causes sodium channels to activate at sub-threshold membrane potentials.

Examination of the sensitivity of BgNa_v1 variants to Lqh-dprIT₃. To identify specific regions of the channel that were involved in the enhanced response to Lqh-dprIT₃, we examined different BgNa_v splice variants. We determined the voltage-dependence of channel activation of nine additional BgNa_v splice variants in the absence or presence of Lqh-dprIT₃ using the same protocol described in Fig. 1A. Since BgNa_v1-1 is a type 1 splice variant, we selected two additional splice variants of that type, BgNa_v1-2 and BgNa_v1-3, and seven variants each representing a different splice type. Besides differences in usage of alternative exons, these variants also contain four to eight unique amino acid changes likely due to RNA editing (25). Strikingly, Lqh-dprIT₃ (300 nM) modified only 14-27% of the channels for all of the other splice variants, compared to 80% for BgNa_v1-1 (Fig. 2A, Table 1), indicating that these variants are less sensitive to Lqh-dprIT₃ than BgNa_v1-1. Dose response analysis revealed that BgNa_v1-1 is 17-fold more sensitive to Lqh-dprIT₃ than

BgNa_v1-3 (Fig. 2B). The toxin-induced hyperpolarizing shift in the voltage-dependence of channel activation ranged from -23 mV to -42 mV (Table 1).

Because the type-1 splice variants BgNa_v1-2 and BgNa_v1-3 were less sensitive to Lqh-dprIT₃ compared to BgNa_v1-1, we reasoned that the alternative exons common to these three variants were not responsible for the hypersensitivity to Lqh-dprIT₃. Compared with BgNa_v1-2 and BgNa_v1-3, four amino acid residues are different in BgNa_v1-1: R502G, L1285P, V1685A and I1806L (Fig. 3). Of these four differences, L1285P and V1685A have been shown to result from U-to-C RNA editing events (25). We examined the effect of Lqh-dprIT₃ on a recombinant channel, BgNa_v1-1a, in which these four unique residues were replaced by those of BgNa_v1-2 and BgNa_v1-3 (25). We found that the sensitivity of BgNa_v1-1a to Lqh-dprIT₃ decreased prominently, with only 18% of the channels modified by 300 nM toxin (Fig. 2, Table 2). This result suggested that one or more of these four amino acids were responsible for the hypersensitivity of BgNa_v1-1 to Lqh-dprIT₃.

L1258P in IIIIS1 is responsible for the hypersensitivity of BgNav1-1 to Lqh-dprIT₃. To determine which of the four amino acid substitutions in BgNa_v1-1 was responsible for the hypersensitivity to Lqh-dprIT₃, we substituted each of the four amino acids in the background of BgNa_v1-1a with those found in BgNa_v1-1 (i.e., R502G, L1285P, V1685A and I1806L) and determined the effect of Lqh-dprIT₃. Whereas none of the substitutions had an effect on the voltage-dependence of channel activation in the absence of toxin (Table 2), 300 nM Lqh-dprIT₃ caused a shift in all four mutant channels (Fig. 3). The fraction of toxin-modified channels was 71% for the L1285P mutant compared to BgNa_v1-1. In contrast, the fraction of toxin-modified channels for the other three mutants was 13-14%, similar to that for BgNa_v1-1a (Fig. 3, Table 2). These results indicated that the L1285P substitution was responsible for the hypersensitivity of BgNa_v1-1 to Lqh-dprIT₃.

To further determine the impact of the side chain of the residue at position 1258 on Lqh-

dprIT₃ action, we substituted L1258 with an aromatic residue (F), two neutral residues (G and C), and a positively-charged K in the background of BgNa_v1-1a. In contrast to L1258P, none of these substitutions increased the channel sensitivity to Lqh-dprIT₃ (Fig. 4, Table 3). In addition, none of these substitutions significantly altered the voltage-dependence of channel activation. However, the L1285G substitution caused a 13 mV positive shift in the voltage-dependence of steady-state inactivation (Data not shown).

Charge reversal or neutralization of a negatively-charged residue, E1290, increased the channel sensitivity to Lqh-dprIT₃. Because of the prominent effect of the L1285P substitution in IIIS1 on Lqh-dprIT₃ action, we analyzed the effect of alanine substitution of two nearby, negatively charged residues (E1290 and D1291) at the extracellular end of IIIS1. E1290 is highly conserved in voltage-gated ion channels including potassium, calcium and sodium channels. The E1290A substitution did not alter the voltage-dependence of activation in the absence of toxin. However, the E1290A channel was also more sensitive to Lqh-dprIT₃ compared to BgNa_v1-1a, similar to the effects of the L1285P substitution. 52% of the E1290A channels were modified by 300 nM Lqh-dprIT₃ versus 18% modified for BgNa_v1-1a (Table 4, Fig. 5). The D1291 substitution by alanine did not alter the channel sensitivity to Lqh-dprIT₃ (data not shown). Because charge neutralization at E1290 enhanced the effect of Lqh-dprIT₃, we further characterized the role of this residue by its substitution with the positively charged amino acid lysine. The E1290K mutation did not alter the voltage-dependence of activation in the absence of toxin, but Lqh-dprIT₃ (300 nM) caused a complete shift of the conductance curve channel by -40 mV (Fig. 5, Table 4).

Effects of reversal of the gating charges in domain III on channel activation and toxin action. To further investigate the role of the voltage-sensing module of domain III in channel sensitivity to Lqh-dprIT₃, we evaluated the effects on toxin action of charge reversal of the five positively charged residues in IIIS4. We individually substituted these residues with

glutamic acid generating K1E, R2E, R3E, R4E and R5E. In the absence of toxin, K1E, R2E, R3E and R4E substitutions caused 5-7 mV negative shifts in the voltage-dependence of activation, whereas the R5E substitution caused a 4 mV positive shift (Table 5). We did not observe a significant change of the slope of the activation curve for K1E, R2E, R3E and R4E channels, although the R5E channel mutant demonstrated a slightly shallower slope compared with that of the parental channel (Table 5, Fig. 6).

The R4E and R5E channel mutants were more sensitive to Lqh-dprIT₃ than BgNa_v1-1a and the K1E, R2E and R3E channel mutants. At 300 nM, the toxin modified over 50% of R4E and R5E channels, but only 18-25% of the other channels. For R5E channels, Lqh-dprIT₃ (300 nM) shifted the voltage dependence of activation of modified R5E channels 40 mV in the hyperpolarizing direction, similar to the extent of the shift for BgNa_v1-1a, K1E, R2E and R3E channels (Fig. 6, Table 5). However, Lqh-dprIT₃ caused a -60 mV shift in voltage dependence of activation for the modified R4E channels, which started to activate at membrane potentials as negative as -100 mV.

DISCUSSION

Differential sensitivities of BgNa_v sodium channel splice-variants from *Blattella germanica* have been valuable in elucidating channel regions involved in channel function and resistance to pyrethroid insecticides (4,5). Here we examined the sensitivity of 10 BgNa_v channel variants to the insect-selective scorpion depressant β -toxin Lqh-dprIT₃. This screening unexpectedly revealed that substitutions at the voltage sensor module of domain III influenced the action of the β -toxin. The binding site of the β -toxin C_{ss}4 has been shown to involve the voltage sensor module of domain II and the pore module of domain III (16,19,31,32). We found that a Leu to Pro substitution at 1285 in IIIS1, resulting from an RNA editing event, was responsible for the hypersensitivity of sodium channel variant BgNa_v1-1 to Lqh-dprIT₃. Further site-directed mutagenesis identified additional residues whose substitution affected the action

of Lqh-dprIT₃, including a negatively charged residue at the extracellular end of IIS1 (E1290) and the two innermost positively charged gating residues in IIS4. Charge reversal of either E1290 or each of the two gating charges in IIS4 did not hinder but rather increased the channel sensitivity to the toxin.

A preliminary 3-D model of C_{ss}4 docking at rNa_v1.2a, constructed using as template the crystal structure of the bacterial voltage-gated potassium channel, K_vAP (21), suggested that the toxin binds at a crevice between S1-S2 and S3-S4 in domain II, thus controlling IIS4 movement during activation. When the two outermost positively-charged residues in IIS4 of rNa_v1.2 residues were neutralized or charge-reversed, C_{ss}4 action increased most likely due to their increased mobility during activation, thus enhancing the trapping by the toxin (31).

The voltage sensing module of domain III has not previously been implicated in the binding and/or action of scorpion β -toxins. The increased sensitivity to Lqh-dprIT₃ by the L1285P and E1290A/K substitutions in IIS1 might indicate that the Lqh-dprIT₃ toxin binds at the crevice juxtaposed to S1 of domain III in the mutant channels. Alternatively, alterations in the domain III may indirectly facilitate trapping of the voltage sensor in domain II by the toxin. The enhanced channel sensitivity to Lqh-dprIT₃ when L1285 was substituted specifically with proline (Table 2) seems more consistent with the latter explanation. Proline inserts a kink in the distal part of the S1 α -helix, which would disrupt the local arrangement of IIS1, including E1290. Since these alterations increased rather than decreased the effect of Lqh-dprIT₃, we speculate that the unmodified IIS1 in BgNa_v1 imposes some structural constraint that limits the full effect of the toxin in binding to the domain II voltage sensor and/or in the voltage-sensor trapping, and this constraint is lifted by the above substitutions.

The most dramatic effect inspected was when the two innermost gating charges in domain III were substituted with negative charges. This result is quite different from the effects of substituting negative charges in the S4

voltage sensor of domain II. In domain II, neutralization of the two outermost charged residues markedly enhanced β -scorpion toxin activation, and neutralization of the three innermost charge residues had no effect (31). In contrast, we observed that reversal of the three outermost charge residues in IIS4 had no effects on toxin activity, and reversal of the two innermost charges greatly enhanced the effect of the toxin. It is unlikely that the two innermost charges directly interact with the toxin because these residues are embedded in the membrane even when the channel is in the activated state. The effects on toxin sensitivity are also unlikely due to effects on the voltage dependence of activation, because the R4E substitution had a similar effect as that of K1E, R1E and R3E substitutions (a hyperpolarizing shift), and the R5E substitution had the opposite effect (a small depolarizing shift). For these reasons, we believe that effects of the R4E and R5E substitutions are most likely mediated by allosteric interactions with the S4 voltage sensor of domain II.

The percentage of modified channels was dependent on the concentration of toxin, whereas the magnitude of the toxin-induced shift in activation was concentration independent. These results suggest that the channels can exist in only two states – unmodified and completely modified. The substitutions in IIS1 (L1285P, E1290A and E1290K) and the R5E substitution in IIS4 increased the percentage of channels that were modified, suggesting that these alterations shifted the equilibrium for toxin modification. In contrast, the R4E substitution in IIS4 increased both the percentage of modified channels and the magnitude of the shift in activation, indicating that this mutation also altered the modified state of the channel. These differential effects are more consistent with an allosteric modulation of channel gating rather than a direct interaction between the substituted residues and the toxin. Bezanilla and associates proposed that the voltage sensors of the sodium channel are intrinsically tightly coupled (33). They have shown that binding of the Ts1 scorpion β -toxin to S4 of domain II allosterically activates the movement of all the other voltage sensors in the sodium channel, with the maximal effect on the neighboring voltage sensors of

domains I and III rather than on the distant S4 of domain IV. Our results suggest that alterations in the voltage sensor of domain III affect this interaction, and that mutations in domain III are likely to enhance the effect of the toxins on domain IIS4. The role of the voltage-sensing module of domain III in the action of Lqh-

dprIT3 on insect sodium channels, as revealed in this study, may be conserved in mammalian sodium channel interaction with other scorpion β -toxins. Future research should test this possibility.

REFERENCES

1. Catterall, W. A. (2000) *Neuron* **26**, 13-25
2. Goldin, A. L. (1999) *Ann N Y Acad Sci* **868**, 38-50
3. Goldin, A. L., Barchi, R. L., Caldwell, J. H., Hofmann, F., Howe, J. R., Hunter, J. C., Kallen, R. G., Mandel, G., Meisler, M. H., Netter, Y. B., Noda, M., Tamkun, M. M., Waxman, S. G., Wood, J. N., and Catterall, W. A. (2000) *Neuron* **28**, 365-368
4. Dong, K. (2007) *Invert Neurosci* **7**, 17-30
5. Dong, K. (2010) *Addendum: Recent Progress in Insect Sodium Channel Research*, Elsevier B. V., Oxford UK
6. Soderlund, D. M. (2010) *Sodium channels*, Elsevier B. V., Oxford UK
7. Catterall, W. A. (1992) *Physiol Rev* **72**, S15-48
8. Gordon, D. (1997b) *Invert Neurosci* **3**, 103-116
9. Nicholson, G. M. (2007) *Toxicon* **49**, 490-512
10. Terlau, H., and Olivera, B. M. (2004) *Physiol Rev* **84**, 41-68
11. Cestèle, S., and Catterall, W. A. (2000) *Biochimie* **82**, 883-892
12. Gordon, D. (1997a) *Sodium channels as targets for neurotoxins: mode of action and interaction of neurotoxins with receptor sites on sodium channels*, Harwood, Amsterdam
13. Martin-Eauclaire, M. F., and Couraud, F. (1995) *Scorpion neurotoxins: effects and mechanisms*, Marcel Dekker, New York
14. Gordon, D., Karbat, I., Ilan, N., Cohen, L., Kahn, R., Gilles, N., Dong, K., Stühmer, W., Tytgat, J., and Gurevitz, M. (2007) *Toxicon* **49**, 452-472
15. Gurevitz, M., Karbat, I., Cohen, L., Ilan, N., Kahn, R., Turkov, M., Stankiewicz, M., Stühmer, W., Dong, K., and Gordon, D. (2007) *Toxicon* **49**, 473-489
16. Cestèle, S., Qu, Y., Rogers, J. C., Rochat, H., Scheuer, T., and Catterall, W. A. (1998) *Neuron* **21**, 919-931
17. Cohen, L., Ilan, N., Gur, M., Stühmer, W., Gordon, D., and Gurevitz, M. (2007) *J Biol Chem* **282**, 29424-29430
18. Leipold, E., Hansel, A., Borges, A., and Heinemann, S. H. (2006) *Mol Pharmacol* **70**, 340-347
19. Marcotte, P., Chen, L. Q., Kallen, R. G., and Chahine, M. (1997) *Circ Res* **80**, 363-369
20. Tsushima, R. G., Borges, A., and Backx, P. H. (1999) *Pflugers Arch Eur J Physiol* **437**, 661-668
21. Cestèle, S., Yarov-Yarovoy, V., Qu, Y., Sampieri, F., Scheuer, T., and Catterall, W. A. (2006) *J Biol Chem* **281**, 21332-21344
22. Armstrong, C. M., and Bezanilla, F. (1977) *J Gen Physiol* **70**, 567-590
23. Hodgkin, A. L., and Huxley, A. F. (1952) *Cold Spring Harb Symp Quant Biol* **17**, 43-52
24. Campos, F. V., Chanda, B., Beirão, P. S., and Bezanilla, F. (2007) *J Gen Physiol* **130**, 257-268
25. Song, W., Liu, Z., Tan, J., Nomura, Y., and K., D. (2004) *J Biol Chem* **279**, 32554-32561
26. Strugatsky, D., Zilberberg, N., Stankiewicz, M., Ilan, N., Turkov, M., Cohen, L., Pelhate, M., Gilles, N., Gordon, D., and Gurevitz, M. (2005) *Biochemistry* **44**, 9179-9187
27. Tan, J., Liu, Z., Nomura, Y., Goldin, A. L., and Dong, K. (2002) *J Neurosci* **22**, 5300-5309
28. Feng, G., Deák, P., Chopra, M., and Hall, L. M. (1995) *Cell* **82**, 1001-1011

29. Warmke, J. W., Reenan, R. A., Wang, P., Qian, S., Arena, J. P., Wang, J., Wunderler, D., Liu, K., Kaczorowski, G. J., Van der Ploeg, L. H., Ganetzky, B., and Cohen, C. J. (1997) *J Gen Physiol* **110**, 119-133
30. Tan, J., Liu, Z., Wang, R., Huang, Z. Y., Chen, A. C., Gurevitz, M., and Dong, K. (2005) *Mol Pharmacol* **67**, 513-522
31. Cestèle, S., Scheuer, T., Mantegazza, M., Rochat, H., and Catterall, W. A. (2001) *J Gen Physiol* **118**, 291-302
32. Cohen, L., Karbat, I., Gilles, N., Ilan, N., Benveniste, M., Gordon, D., and Gurevitz, M. (2005) *J Biol Chem* **280**, 5045-5053
33. Chanda, B., Asamoah, O. K., and Bezanilla, F. (2004) *J Gen Physiol* **123**, 217-230

FOOTNOTES

This work was supported in part by a United States-Israel Binational Agricultural Research and Development Grant IS-4066-07 (to D.G., M.G. and K.D.), a US National Science Foundation Grant IBN 9808156 to K.D, a US National Institutes of Health Grant GM057440 to K.D., and the Israeli Science Foundation Grant 107/08 (to M.G. and D.G.).

FIGURE LEGENDS

FIGURE 1. Effects of Lqh-dprIT₃ on the BgNa_v1-1 sodium channel. *A*, Sodium current traces in the absence (left) and presence (right) of Lqh-dprIT₃ (300 nM). To measure the effect of Lqh-dprIT₃, the following protocol was used: a 20-Hz train of 50 5-ms depolarizing prepulses to 50 mV as the conditional pulses followed by a series of 20-ms depolarizing test pulses between -80 mV and -65 mV. The holding potential was -120 mV. *B* and *C*, Current-voltage relationships in the absence (solid circles) and the presence of Lqh-dprIT₃ (100 nM, triangles, 300 nM, squares) without (*C*) or with (*B*) the conditional depolarizing pulses. *D*, Conductance-voltage relationships in the absence (solid circles) and the presence of Lqh-dprIT₃ (100 nM, triangles, 300 nM, squares) with the conditional depolarizing pulses. The voltage-dependence of activation was measured using the protocol described in Experimental Procedures.

FIGURE 2. Effect of Lqh-dprIT₃ on 10 BgNa_v variants. *A*, Conductance-voltage relationships in the absence (solid circles) and presence of Lqh-dprIT₃ (300 nM, open circles) of eight BgNa_v variants and a recombinant BgNa_v1-1a originated from BgNa_v1-1. Conductance-voltage relationship was measured using the protocol described in Experimental Procedures. *B*, Dose response curve of BgNa_v1-3 in comparison with BgNa_v1-1. *C*, Conductance-voltage relationship in the absence (solid circles) and presence of Lqh-dprIT₃ (300 nM, open circles) of a recombinant BgNa_v1-1a originated from BgNa_v1-1. Four amino acid changes in BgNa_v1-1 were corrected by site-directed mutagenesis generating BgNa_v1-1a (25).

FIGURE 3. L1285P is responsible for the hypersensitivity of BgNa_v1-1 to Lqh-dprIT₃. *A*, Four amino acid changes in BgNa_v1-1 are indicated in the topology of the BgNa_v sodium channel protein. *B*, Conductance curves in the absence (solid circles) and presence of Lqh-dprIT₃ (300 nM, open circles) of four mutant BgNa_v1-1a channels. Each of the four mutations was introduced into the BgNa_v1-1a channel. Conductance-voltage relationship was measured using the protocol described in Experimental Procedures.

FIGURE 4. Substitutions of L1285 with other residues did not alter the hypersensitivity of BgNa_v1-1 to Lqh-dprIT₃. Conductance curves in the absence (solid circles) and presence of Lqh-dprIT₃ (300 nM, open circles) of four mutant BgNa_v1-1a channels with different side chain substitutions at 1285.

Conductance-voltage relationship was measured using the protocol described in Experimental Procedures.

FIGURE 5. Neutralization and charge reversal of E1290 enhanced the channel sensitivity to Lqh-dprIT₃. Conductance curves in the absence (solid circles) and presence of Lqh-dprIT₃ (300 nM, open circles). Conductance-voltage relationship was measured using the protocol described in Experimental Procedures.

FIGURE 6. Effects of charge reversal of the five positively charged residues in IIS4 on the action of Lqh-dprIT₃. Conductance curves in the absence (solid circles) and presence of Lqh-dprIT₃ (300 nM, open circles). Conductance-voltage relationship was measured using the protocol described in Experimental Procedures.

Table 1. Voltage dependence of activation of BgNa_v splice variants before and after the application of 300 nM Lqh-dprIT₃

	Toxin-free		Lqh-dprIT ₃ (300 nM)					
	V _{0.5}	k ₁	V _{0.5}	k ₁	A ₁ (%)	V _{0.5}	k ₂	A ₂ (%)
BgNa _v 1-1	-23.2 ± 1.0	6.3 ± 0.3	-21.0 ± 0.4	5.3 ± 0.3	20 ± 5*	-62.8 ± 2.6	7.9 ± 0.5	80 ± 5*
BgNa _v 1-1a	-28.4 ± 2.1	4.1 ± 0.6	-28.1 ± 1.5	5.0 ± 0.3	82 ± 5	-60.0 ± 3.3	10.4 ± 1.6	18 ± 5
BgNa _v 1-2	-25.2 ± 2.8	5.1 ± 1.1	-25.5 ± 2.1	6.1 ± 1.4	81 ± 3	-58.1 ± 1.2	8.6 ± 0.8	19 ± 3
BgNa _v 1-3	-30.4 ± 2.1	4.3 ± 0.6	-30.6 ± 1.5	5.5 ± 0.4	86 ± 4	-68.7 ± 0.8	5.4 ± 0.3	14 ± 4
BgNa _v 5	-35.9 ± 2.6	3.7 ± 0.5	-35.7 ± 0.7	4.0 ± 0.4	77 ± 1	-59.3 ± 3.0	11.5 ± 0.9	23 ± 1
BgNa _v 6	-27.9 ± 2.4	4.1 ± 0.9	-29.2 ± 2.6	5.2 ± 0.9	79 ± 5	-59.0 ± 5.8	10.9 ± 2.3	21 ± 3
BgNa _v 7	-31.7 ± 1.9	4.8 ± 0.4	-32.5 ± 2.3	3.1 ± 0.6	79 ± 6	-56.7 ± 2.8	11.8 ± 2.1	21 ± 5
BgNa _v 8	-26.5 ± 1.0	4.8 ± 0.2	-26.2 ± 0.9	5.5 ± 0.2	86 ± 3	-60.0 ± 0.5	8.2 ± 0.2	14 ± 3
BgNa _v 9	-30.7 ± 3.1	6.4 ± 1.2	-31.0 ± 2.9	7.5 ± 1.4	82 ± 5	-60.0 ± 2.6	10.1 ± 1.5	18 ± 5
BgNa _v 10	-34.1 ± 2.4	3.5 ± 0.5	-35.8 ± 0.7	3.9 ± 0.7	75 ± 6	-58.6 ± 2.0	14.3 ± 2.6	25 ± 6
BgNa _v 11	-49.3 ± 2.0	-3.2 ± 0.5	-43.2 ± 2.7	5.6 ± 0.7	73 ± 3	-73.7 ± 3.0	2.9 ± 1.1	27 ± 3

Each value represents the mean ± S.D. for at least five oocytes. The asterisks indicate significant differences from other splice variants (p < 0.05).

Table 2. Voltage dependence of activation of BgNa_v1-1a and mutants before and after the application of 300 nM Lqh-dprIT₃

	Toxin-free		Lqh-dprIT ₃ (300 nM)					
	V _{0.5}	k	V _{0.5}	k ₁	A ₁ (%)	V _{0.5}	k ₂	A ₂ (%)
BgNa _v 1-1a	-28.4 ± 2.1	4.1 ± 0.6	-28.1 ± 1.5	5.0 ± 0.3	82 ± 5	-60.0 ± 3.3	10.4 ± 1.6	18 ± 5
R502G	-28.3 ± 0.6	4.0 ± 0.2	-27.5 ± 1.3	5.1 ± 0.1	86 ± 2	-60.0 ± 3.5	11.6 ± 1.5	14 ± 2
L1285P	-25.0 ± 1.0	5.4 ± 0.2	-25.1 ± 1.6	5.5 ± 0.5	29 ± 4*	-64.3 ± 1.5	8.6 ± 0.9	71 ± 4*
V1685A	-27.5 ± 0.7	3.9 ± 0.2	-26.0 ± 1.5	4.7 ± 0.3	86 ± 4	-61.3 ± 2.0	7.4 ± 1.0	14 ± 4
I1806L	-26.2 ± 0.5	4.4 ± 0.3	-24.6 ± 1.2	5.1 ± 0.2	87 ± 3	-63.5 ± 2.0	6.6 ± 0.8	13 ± 3

Each value represents the mean ± S.D. for at least five oocytes. The asterisks indicate significant differences from BgNa_v1-1a (p < 0.05).

Table 3. Voltage dependence of activation of BgNa_v1-1a and L1285 substations before and after the application of 300 nM Lqh-dprIT₃

	Toxin-free		Lqh-dprIT ₃ (300 nM)					
	V _{0.5}	k	V _{0.5}	k ₁	A ₁ (%)	V _{0.5}	k ₂	A ₂ (%)
BgNa _v 1-1a	-28.4 ± 2.1	4.1 ± 0.6	-28.1 ± 1.5	5.0 ± 0.3	82 ± 5	-60.0 ± 3.3	10.4 ± 1.6	18 ± 5
L1285P	-25.0 ± 1.0	5.4 ± 0.2	-25.1 ± 1.6	5.5 ± 0.5	29 ± 4*	-64.3 ± 1.5	8.6 ± 0.9	71 ± 4*
L1285F	-28.6 ± 1.1	4.2 ± 0.2	-25.0 ± 1.0	4.8 ± 0.2	87 ± 4	-61.6 ± 3.1	8.3 ± 0.2	13 ± 4
L1285G	-28.7 ± 0.8	3.9 ± 0.3	-27.8 ± 1.2	4.0 ± 0.6	85 ± 3	-50.6 ± 6	10.1 ± 2.0	15 ± 3
L1285K	-30.5 ± 2.1	4.6 ± 0.4	-27.5 ± 1.5	5.9 ± 0.6	86 ± 2	-67.2 ± 1.9	8.5 ± 1.2	14 ± 2
L1285C	-28.7 ± 0.3	4.1 ± 0.3	-25.9 ± 1.6	4.6 ± 0.2	85 ± 2	-59.6 ± 3.1	11.0 ± 1.6	15 ± 2

Each value represents the mean ± S.D. for at least five oocytes. The asterisks indicate significant differences from BgNa_v1-1a (p < 0.05).

Table 4. Voltage dependence of activation of BgNa_v1-1a and mutants before and after the application of 300 nM Lqh-dprIT₃

	Toxin-free		Lqh-dprIT ₃ (300 nM)					
	V _{0.5}	k ₁	V _{0.5}	k ₁	A ₁ (%)	V _{0.5}	k ₂	A ₂ (%)
BgNa _v 1-1a	-28.4 ± 2.1	4.1 ± 0.6	-28.1 ± 1.5	5.0 ± 0.3	82 ± 5	-60.0 ± 3.3	10.4 ± 1.6	18 ± 5
E1290A	-24.5 ± 1.8	4.9 ± 0.3	-24.0 ± 3.5	6.9 ± 0.2	48 ± 12*	-60.0 ± 2.4	6.1 ± 0.5	52 ± 12*
E1290K	-24.2 ± 1.2	6.6 ± 0.4				-68.1 ± 2.8	7.5 ± 0.4	

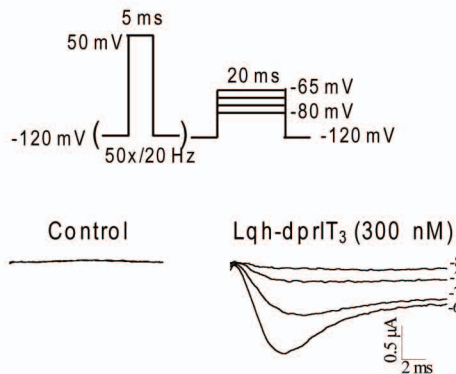
Each value represents the mean ± S.D. for at least five oocytes. The asterisks indicate significant differences from BgNa_v1-1a (p < 0.05).

Table 5. Voltage dependence of activation of BgNa_v1-1a and mutants before and after the application of 300 nM Lqh-dprIT₃

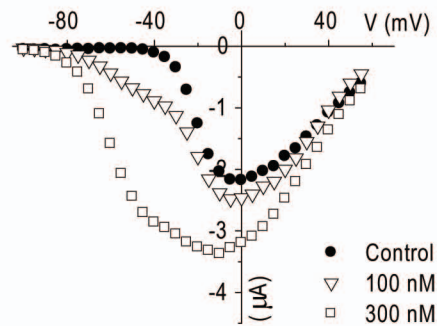
	Toxin-free		Lqh-dprIT ₃ (300 nM)					
	V _{0.5}	k ₁	V _{0.5}	k ₁	A ₁ (%)	V _{0.5}	k ₂	A ₂ (%)
BgNa _v 1-1a	-28.4 ± 2.1	4.1 ± 0.6	-28.1 ± 1.5	5.0 ± 0.3	82 ± 5	-60.0 ± 3.3	10.4 ± 1.6	18 ± 5
K1E	-35.5 ± 2.5	4.7 ± 0.4	-35.8 ± 3.9	4.8 ± 0.3	82 ± 4	-70.0 ± 6.1	10.7 ± 2.1	18 ± 4
R2E	-34.3 ± 2.8	5.1 ± 0.3	-32.9 ± 2.1	5.5 ± 0.4	81 ± 4	-75.5 ± 4.5	7.4 ± 0.8	19 ± 4
R3E	-34.2 ± 2.5	5.0 ± 0.2	-34.7 ± 2.7	6.8 ± 0.3	75 ± 5	-76.1 ± 8.7	7.0 ± 0.6	25 ± 5
R4E	-33.7 ± 3.8	5.7 ± 0.5	-26.9 ± 3.6	8.1 ± 0.6	43 ± 8*	-87.9 ± 3.6	5.1 ± 0.5	57 ± 8*
R5E	-24.0 ± 1.9	7.2 ± 0.4	-25.0 ± 3.9	8.6 ± 0.8	35 ± 7*	-63.6 ± 5.0	7.9 ± 0.6	65 ± 7*

The asterisks indicate significant differences from BgNa_v1-1a (p < 0.05).

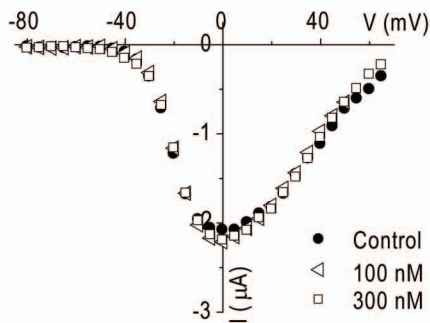
A



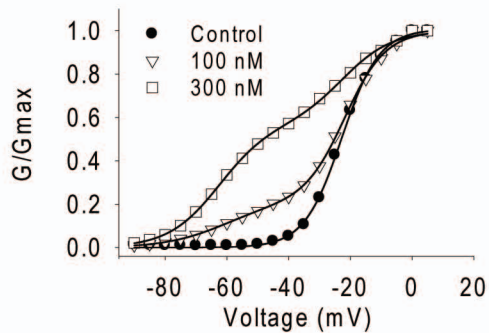
B



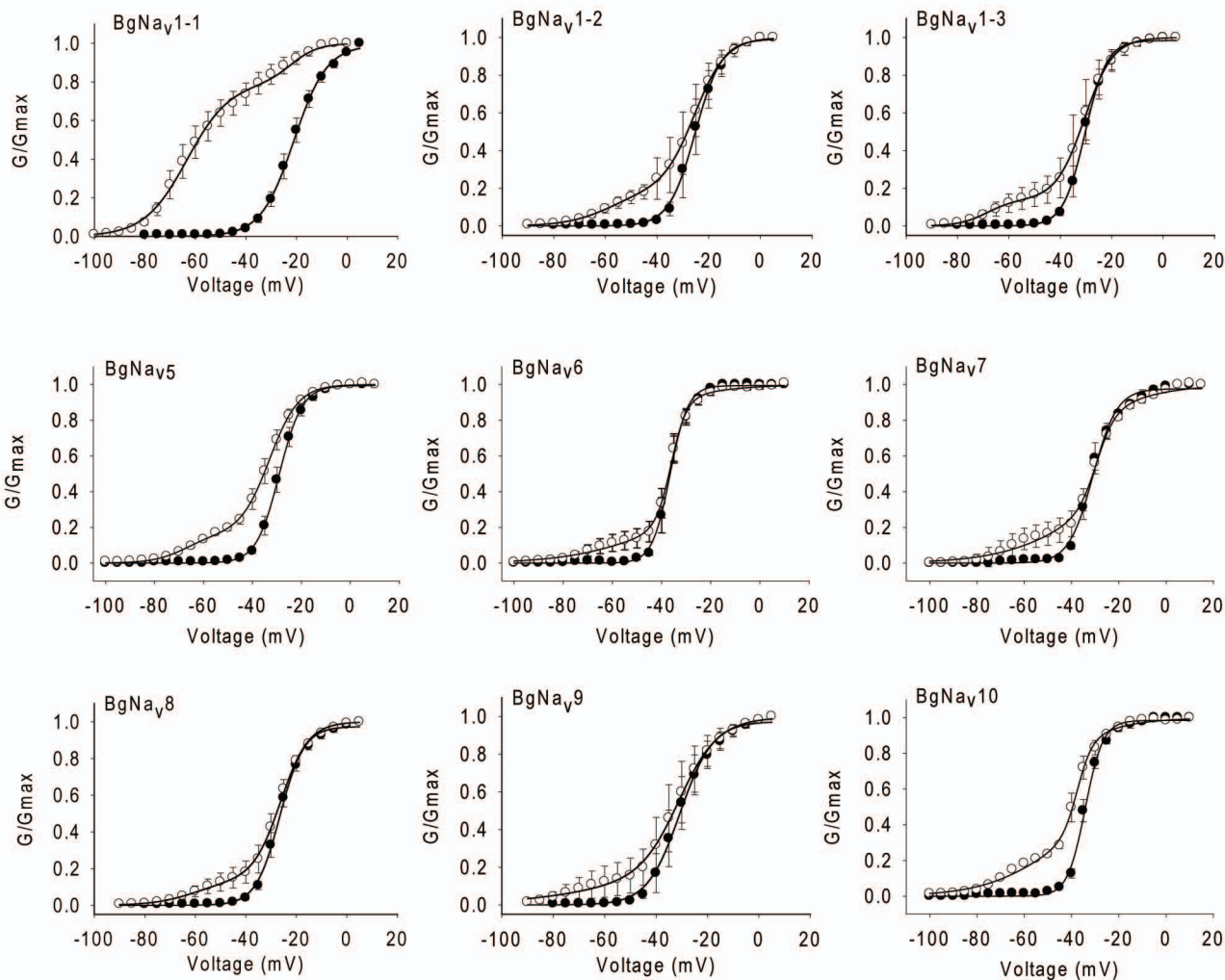
C



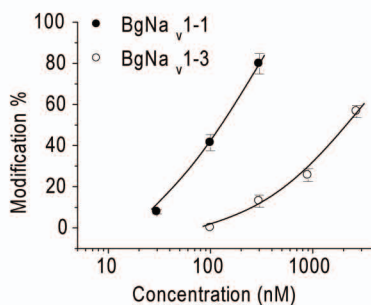
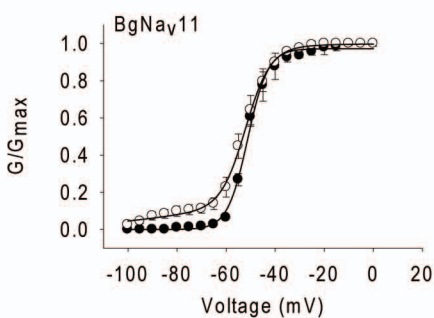
D



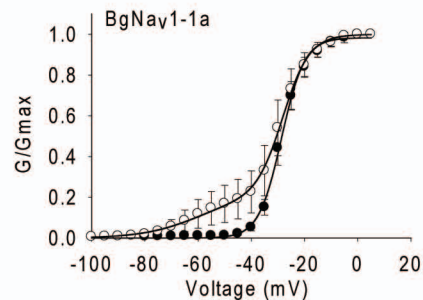
A



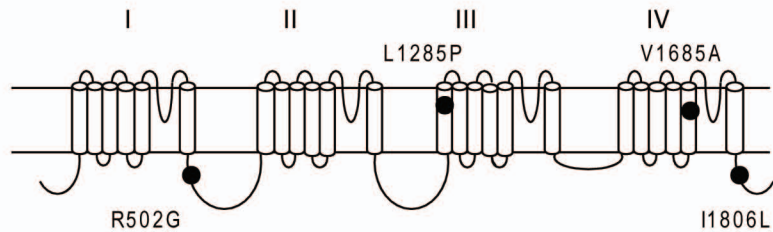
B



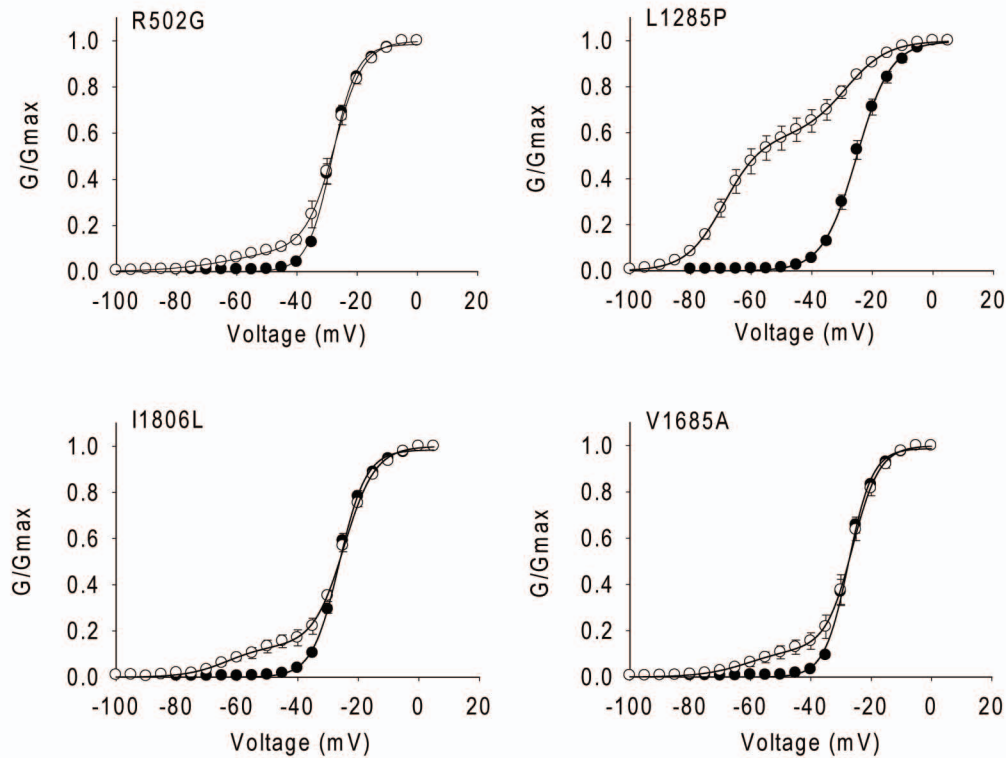
C

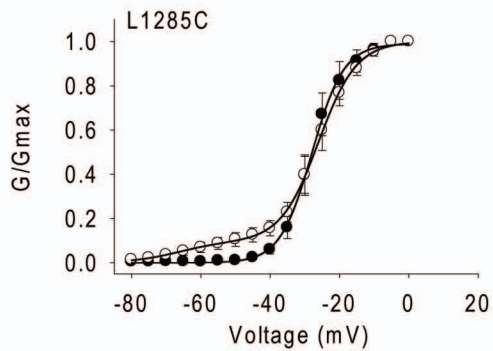
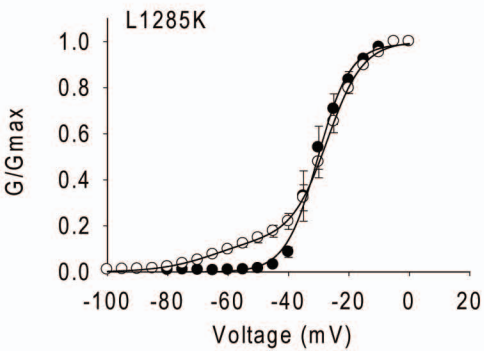
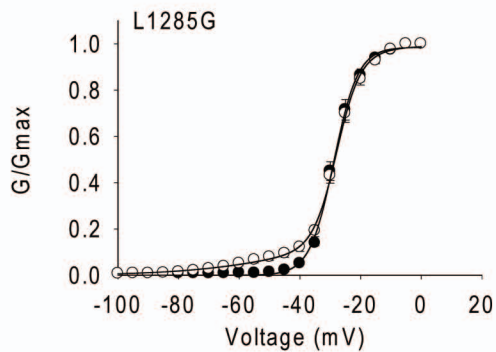
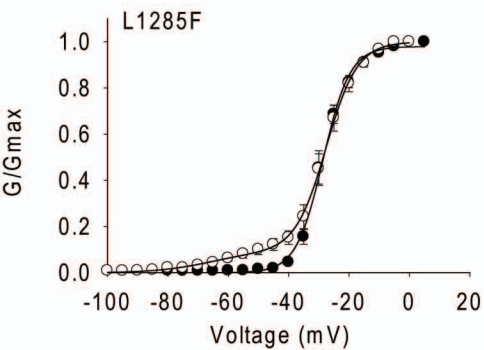


A

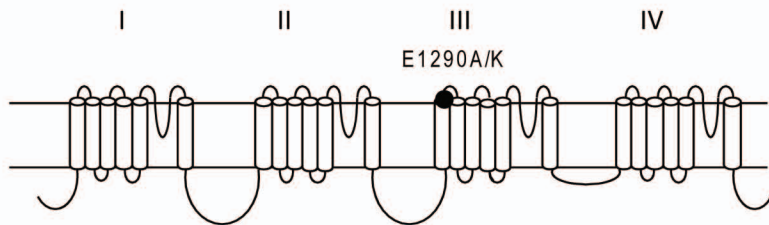


B





A



B

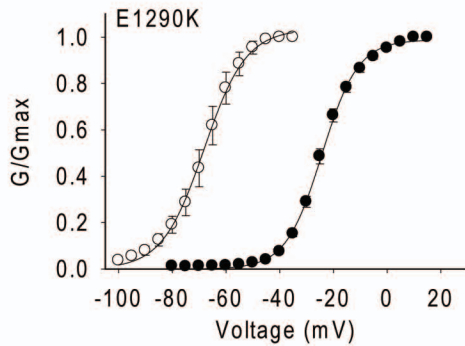
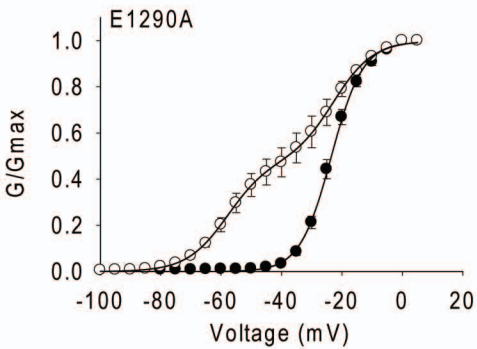


Fig. 6

